Sigma J Eng & Nat Sci 37 (4), 2019, 1199-1206

Sigma Journal of Engineering and Natural Sciences
Sigma Mühendislik ve Fen Bilimleri Dergisi

Research Article

STRUCTURAL CHARACTERIZATION OF ACID AND BASE-CATALYZED SILICA XEROGELS

Eda KELEŞ GÜNER[1], Abdulkadir ÖZER*[2]

[1]*Department of Civil Defense and Firefighting, Üzumlu Vocational School, Erzincan University, ERZINCAN;* ORCID: 0000-0001-4421-1315
[2]*Department of Chemical Engineering, Ataturk University, ERZURUM;* ORCID: 0000-0001-0487-3680

Received: 09.04.2019 Revised: 14.06.2019 Accepted: 16.08.2019

ABSTRACT

In this study, silica xerogels were synthesized by the sol gel method using TEOS (tetraethyl orthosilicate), ethanol, water and sulfuric acid as acidic catalyst and ammonia as basic catalyst. The structural characterizations of the synthesized acid-catalyzed silica xerogels (ACXs) and base-catalyzed silica xerogels (BCXs) were investigated by thermal gravimetric analysis (TGA), scanning electron microscopy (SEM) and N_2 adsorption and desorption techniques. It was seen from TGA analyzes that the thermal decomposition process of silica xerogels consists of two steps. The SEM images show that the solid skeletal phase of ACXs has a globular morphology with primary particles that are joined together to form agglomerates. In contrast, SEM images of the BCXs indicate a hierarchical morphology with the clusters of these agglomerates organized into larger spherical particles. The pore size distributions (PSD) of ACXs and BCXs samples show a main peak in the micropore and micro-mesopore regions, respectively.
Keywords: Silica xerogels, sol-gel method, microporous materials, pore structure.

1. INTRODUCTION

The synthesis of inorganic materials using sol-gel techniques is an active field of research worldwide. The sol–gel process is an attractive method for synthesizing porous materials with controllable surface and structural properties. In addition, the sol-gel process is highly efficient due to the low temperature of the chemical process, high homogeneity, and products purity [1,2]. The most significant commercial products currently prepared using sol-gel methods are in the areas of optical coatings, refractory ceramic fibers, and several specialized applications ranging from insulation to semiconductor manufacturing [3-5].

Tetraethyl orthosilicate (TEOS) is widely used for a raw material of high purity silicon dioxide of extremely low alkaline and other metal content by careful distillation followed by hydrolysis and calcination [6-7]. The sol–gel process consists of hydrolysis and condensation of alkoxide precursor. In sol–gel process, a sol is first formed by mechanically mixing a liquid alkoxide precursor, such as TEOS, water, a co solvent, and an acid or base catalyst at room temperature. During this step, alkoxide groups are removed by acid- or base-catalyzed hydrolysis

* Corresponding Author: e-mail: kadirozer@atauni.edu.tr, tel: (442) 231 45 85

reactions [8]. The resulting sol is cast into a mold, whereupon gelation causes a solid in the shape of the mold to be formed. The gel is aged (syneresis) in the pore liquid for a period of time to allow the gel network to strengthen. The gel is then dried under atmospheric conditions to remove the liquid. The obtained porous silica is called silica xerogels [9,10]. Silica xerogels have a wide range of application fields, such as insulation [11], catalysis [12], controlled drug release [13] and bioencapsulation [14], which depend directly on their physical properties and on the variety of nanostructures attainable. These materials consist in a three-dimensional SiO_2 network obtained by the sol–gel process [15-17].

In this work, silica xerogels were synthesized using H_2SO_4 as a different acidic catalyst other than the literature and NH_3 as basic catalyst for comparison the structural changes between synthesized both sample. The structural properties of the acid-catalyzed silica xerogels (ACXs) and base-catalyzed silica xerogels (BCXs) were investigated by thermogravimetric analysis (TGA), scanning electron microscopy (SEM) and nitrogen adsorption–desorption measurements.

2. EXPERIMENTAL

2.1. Synthesis of silica xerogels

Tetraethyl orthosilicate (TEOS) was used as silica source, ethanol as solvent and as acidic catalyst H_2SO_4 and basic catalyst NH_3. Deionized water was also used. The molar ratios of TEOS, ethanol, water and catalyst were 1:4:4:0.67. Synthesis of the silica xerogels by sol–gel process was made in polypropylene container at room temperature, under atmospheric pressure. The ACXs and BCXs were synthesized, aged and dried according to the procedure schematized in Fig. 1.

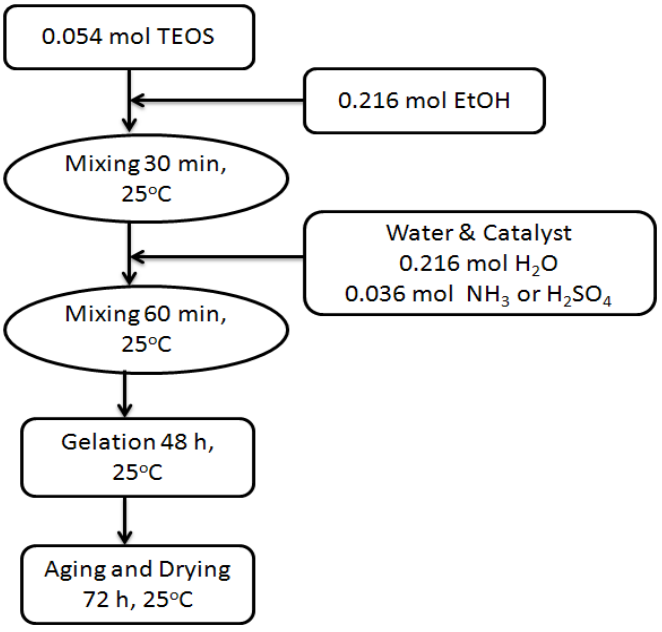

Figure 1. Schematic representation of the synthesis steps of the acid and base-catalyzed silica xerogels

2.2. Characterization of silica xerogels

The amount of silanol groups adsorbed on the surface of silica xerogels was investigated by using TGA analyzer (NETZSCH STA 409 PC Luxx) in air at a heating rate of 10°C/min. N_2 adsorption and desorption isotherms were measured at -196°C using a Quantachrome Autosorb-1 C instrument. Prior to N_2-physisorption measurements, the products were degassed at 200°C for 12 h. The structural variables used to characterize the pores in these xerogels, such as the pore volume, specific surface area, pore distribution and average pore diameter were determined from the N_2 adsorption-desorption data. The volume of N_2 required to fill the pores at relative pressures approaching unity indicated the pore volumes. The specific surface areas were obtained by fitting the adsorption isotherms to the Brunauer-Emmett-Teller (BET) equation [18]. Pore distributions and average pore diameters were calculated from the desorption isotherms using the Barrett-Joyner-Halenda (BJH) method [19]. The surface morphology and the pore structure of silica xerogels were analyzed by using scanning electron microscopy (FEI-Nova Nanosem 430, FEI Inspect F 50 with Au-coated, operated at 20 keV).

3. RESULTS AND DISCUSSION

Fig. 2 shows TGA patterns of synthesized ACXs and BCXs samples. It was found that the TGA patterns of silica xerogels consisted of two steps of weight losses at the temperatures below 200°C and above 300°C. The first step was attributed to physically and chemically adsorbed water molecules and to the evaporation of the remnant alcohol in macropores and micropores, respectively. At the first stage, the larger weight loss in ACXs in these temperature ranges suggests that the samples ACXs have larger pore volume (micropore and macropore) than those in samples BCXs. At the second step, weight loss above 300°C corresponds to the elimination of residual organic groups. The larger weight loss of the ACXs in these temperature range indicates that a larger amount of residual organic groups existed in the ACXs.

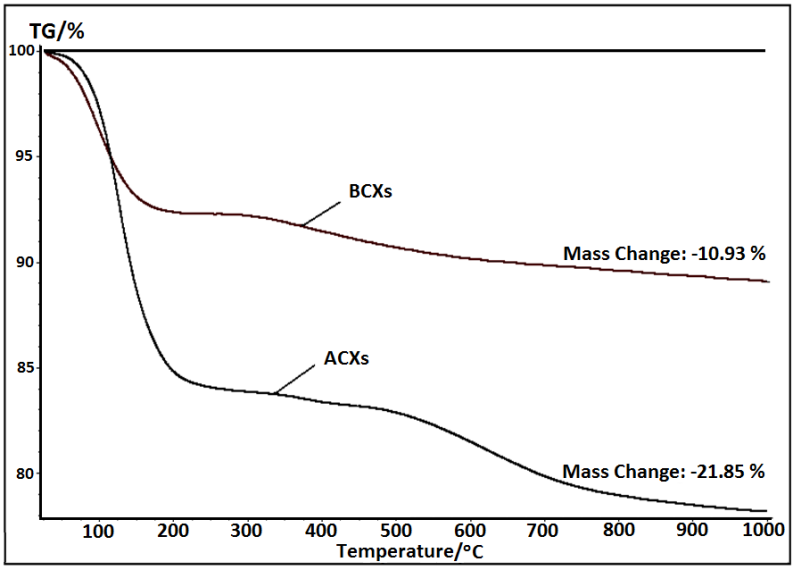

Figure 2. TGA curves of samples ACXs and BCXs

The surface morphology and chemical composition of the acid-catalyzed and base-catalyzed xerogels prepared by the sol-gel method are investigated by SEM combined with EDS shown in Figs. 3 and 4, respectively. According to the SEM images can be seen that the morphology of each sample to another clearly different. SEM images (Fig. 3) revealed the smooth and dense surface of ACXs caused by an aggregation of fine silica nanoparticles. The SEM image shows that the microstructure of the ACXs is a consolidation of these agglomerates. It is show that the solid skeletal phase has a globular morphology with primary particles, 30–70 nm in diameter, that are joined together to form agglomerates. The agglomerates are smaller and more closely packed in the ACXs. In contrast, the SEM images (Fig. 4) of the BCXs indicate a hierarchical morphology with the clusters of these agglomerates organized into larger spherical particles approaching 200-250 nm in diameter. The EDS spectrum detected the Si and O atoms without any other unknown impurity (Fig.5).

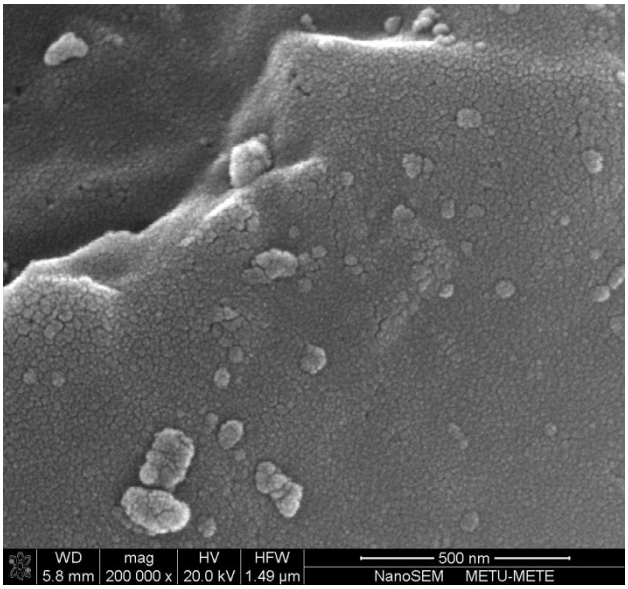

Figure 3. SEM micrographs acid-catalyzed xerogels

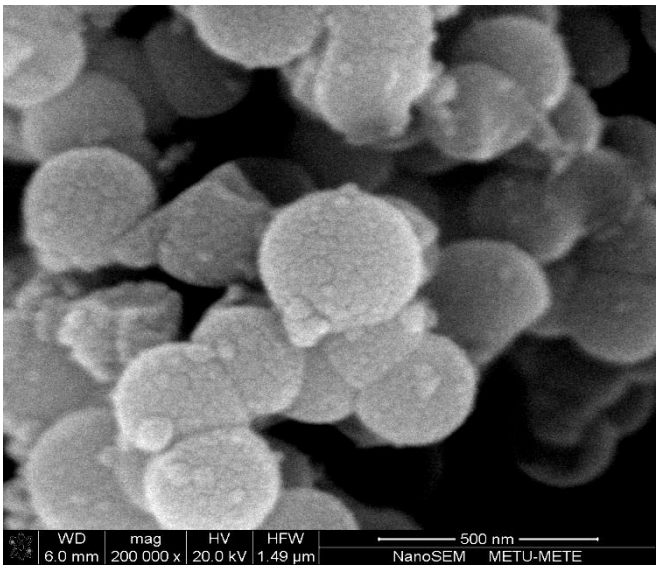

Figure 4. SEM micrographs base-catalyzed xerogels

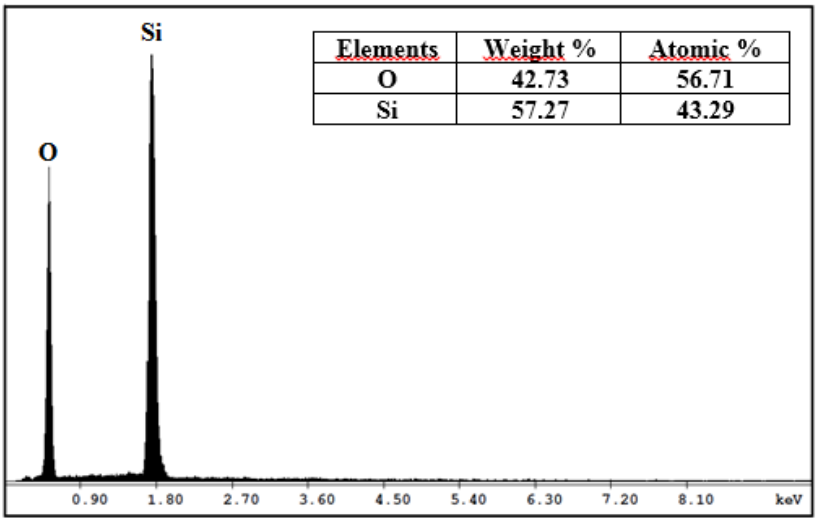

Elements	Weight %	Atomic %
O	42.73	56.71
Si	57.27	43.29

Figure 5. EDS image of acid and base-catalyzed xerogels

Adsorption–desorption isotherms of the ACXs and BCXs samples as function of P/P_0, where P is the adsorbate equilibrium pressure and P_0 is the adsorbate saturated equilibrium vapor pressure, are presented in Fig. 6. It is seen from Fig. 6 that the ACXs has more the micropores than the BCXs at the low values of P/P_0. On the other hand, the ACXs show the appearance of hysteresis at the intermediate values P/P_0. The ACXs presented a type-I adsorption–desorption isotherm and H4 hysteresis loop characteristic of microporous materials by BDDT/IUPAC classification [20]. It can be concluded that the pore structure can be the ink-bottle. The ACXs is

indicative of materials of uniform spheroid particles that tend to possess a narrow pore size range. This was a confirmed characteristic of the ACXs by the presence of approximately uniform spheroid particles shown by the SEM images in Fig. 3. The BCXs shows isotherms characteristic of intermediate porosity materials, whose profiles changed to a typical type-IV adsorption–desorption isotherm and H3 hysteresis loop. The BCXs also possesses spheroid particles, but of larger size. As spheroid particles grow larger, pores become less cylindrical and more undefined which could result in a little change in hysteresis shape.

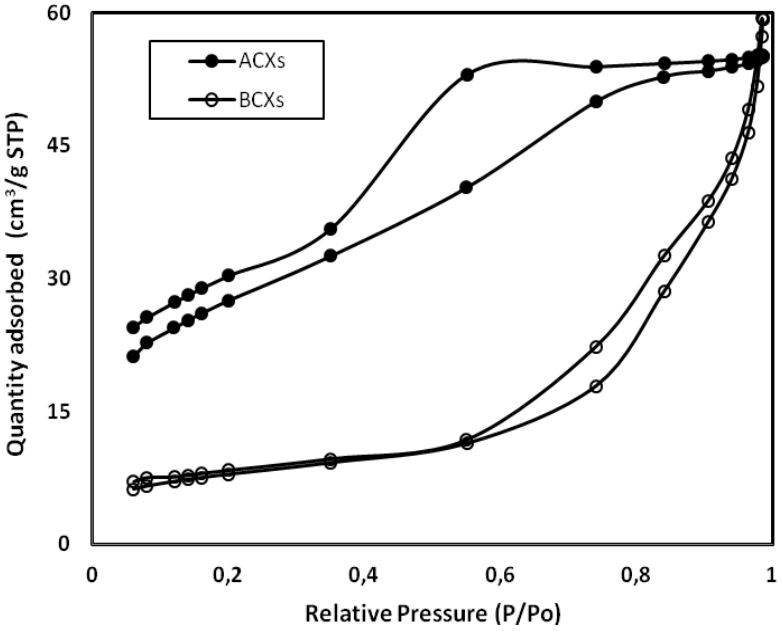

Figure 6. The nitrogen adsorption-desorption isotherms of the ACXs and BCXs samples

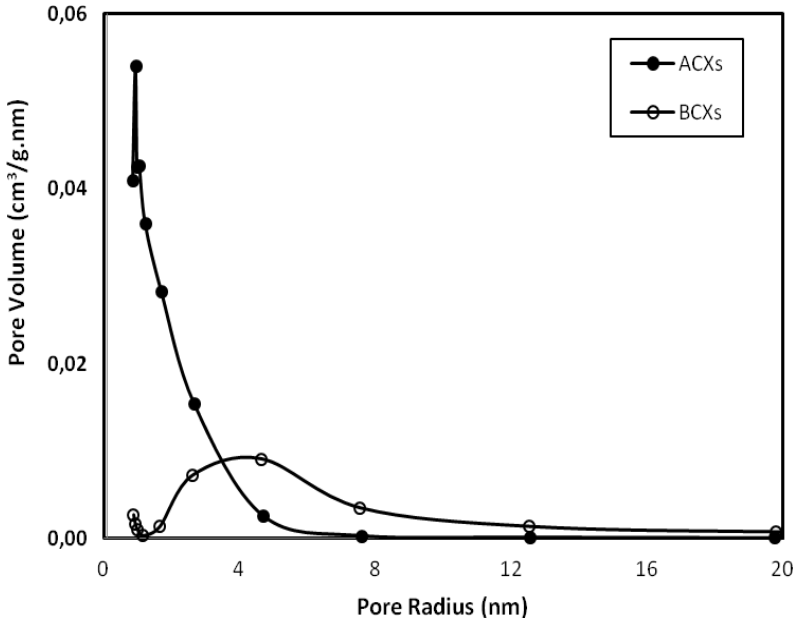

Figure 7. Pore size distributions of the ACX and BCX samples

The pore size distribution is an important parameter for porous materials. Pore size distributions determined by the BJH method for the ACXs and BCXs are shown in Fig. 7. For ACXs, the pore distribution rapidly decreases with increasing pore diameter. This distribution gives an average pore diameter of 1.75 nm. For BCXs, the shape of this distribution is consistent with a microstructure composed of micropores and mesopores. This distribution gives an average pore diameter of 6.24 nm. The micropore volume of ACXs is greater than BCXs. The micropore volume of the ACXs is 0.0042cm^3/g; BCXs is 0.0017cm^3/g. On the other hand, the total pore volumes of ACXs and BCXs are 0.0924 and 0.0855 cm^3/g, respectively. A BET analysis of the adsorption data gives surface areas of 99.53 m^2/g for ACXs and 28.35 m^2/g for BCXs.

4. CONCLUSIONS

The structural characterizations of the ACXs and BCXs synthesized by the sol gel method were investigated by TGA, SEM and BET techniques. It was found that the TGA patterns of silica xerogels consisted of two steps. At the first stage, the weight loss of sample BCXs is much lower than that of sample ACXs. The SEM images show that the solid skeletal phase of ACXs has a globular morphology with primary particles, 30–70 nm in diameter, that are joined together to form agglomerates. In contrast, SEM images of the BCXs indicate a hierarchical morphology with the clusters of these agglomerates organized into larger spherical particles approaching 200-250 nm in diameter. The surface areas (BET) of the ACXs and BCXs are 99.53 and 28.35 m^2/g, respectively. The micropore volume of ACXs is greater than BCXs. The pore size distributions (PSD) of ACXs and BCXs gives an average pore diameter of 1.75 and 6.24 nm, respectively.

REFERENCES

[1] Brinker, C.J., Scherer, G.W. (1990) *Sol-gel Science: the physics and chemistry of Sol-Gel processing*, Academic Press. New York, 19901.

[2] Zarzycki, J. (1997) Past and Present of Sol-Gel Science and Technology, *Journal of Sol-Gel Science and Technology* (8), 17-22.

[3] Uhlmann, D.R. (1997) The Future of Sol-Gel Science and Technology, *Journal of Sol-Gel Science and Technology* (8), 1083-1091.

[4] Klein, L.C. (1988) Sol-Gel Technology for Thin Films, Fibers, Preforms, Electronics and Specialty Shapes, *Noyes Publications, Park Ridge, NJ*.

[5] Verganelakis, V., Nicolaou, P.D., Kordas, G. (2000) Processing and properties of glass strengthened by Ormosil coatings. *Glass technology*, (41), 22-29.

[6] Scherdel, C., Reichenauer, G. (2015) Highly porous silica xerogels without surface modification. *The Journal of Supercritical Fluids*, *106*, 160-166.

[7] Ferauche, F., Winterton, N., & Alié, C. (2006). Characterization of low-density silica xerogel formed into microspheres. *Journal of non-crystalline solids*, *352*(1), 8-17.

[8] Bryans, T.R., Brawner, V.L., Quiteves, E.L., (2000) Microstructure and Porosity of Silica Xerogel Monoliths Prepared by the Fast Sol-Gel Method, *Journal of Sol-Gel Science and Technology* (17), 211–217.

[9] Brinker, C.J., Scherer, G.W., (1990) Sol–Gel Science, The Physics and Chemistry of Sol–Gel Processing, *Academic Press*, *New York*.

[10] Filipovic, R., Obrenovic, Z., Stijepovic, I., Nikolic, L.M., Srdic, V.V., (2009) Synthesis of mesoporous silica particles with controlled pore structure, *Ceramics Int.* (35), 3347–3353.

[11] Pajonk, G.M. (2003) Some applications of silica aerogels, *Colloid Polymer Science* (281), 637–651.

[12] Tillotson, T.M., Reynolds, J.G. (2003) Structure and characterization of sol-gel and aerogel materials and oxidation products from the reaction of $(CH_3O)_4Si$ and $C_{16}H_{33}Si(OCH_3)_3$, *Journal of Non-Crystalline Solids* (331), 168-176.

[13] Kortesuo, P., Ahola, M., Kangas, M., Yli-Urpo, A., Kiesvaara, J., Marvola, M. (2001) In vitro release of dexmedetomidine from silica xerogel monoliths: effect of sol-gel synthesis parameters, *International Journal of pharmaceutics* (221), 107-114.

[14] Luckarift, H.R., Spain, J.C., Naik, R.R., Stone, M.O. (2004) Enzyme immobilization in a biomimetic silica support, *Nature Biotechnology* (22), 211–213.

[15] Iller, R.K. (1979) The Chemistry of Silica, *Wiley-Interscience*, *NewYork.*

[16] Sakai, N., Nakano, T., Yanaba, K., Imazeki, S. (2018) Studies of the characteristic and reaction mechanism of silica xerogel by sol–gel method catalyzed by alkylbiguanide as a strong organic base. *Journal of Sol-Gel Science and Technology* 88 (2), 379-385.

[17] de Miranda, L.A., Mohallem, N.D., de Magalhães, W.F. (2006) Morphological and textural characterization of functionalized particulate silica xerogels. *Applied surface science* 252 (10), 3466-3474.

[18] Brunauer, S., Deming, L.S., Deming, W.E., Teller, E. (1940) On a theory of the van der Waals adsorption of gases, *Journal of American Chemical Society* (62), 1723.

[19] Barrett, E.P., Joyner, L.G., Halenda, P.P. (1951) The determination of pore volume and area distributions in porous substances. I. Computations from nitrogen isotherms, *Journal of American Chemical Society* (73), 373–380.

[20] S.J. Gregg, K.S.W. Sing, (1982) *Adsorption, Surface Area and Porosity*, Academic Press Inc., San Diego.